Recent developments of human monocarboxylate transporter (*h*MCT) inhibitors as anticancer agents

Puhua Wu[1], Yan Zhou[1], Yizhen Guo[1], Shao-Lin Zhang[2] and Kin Yip Tam[1]

[1] Cancer Centre, Faculty of Health Sciences, University of Macau, Macau
[2] Chongqing Key Laboratory of Natural Product Synthesis and Drug Research, School of Pharmaceutical Sciences, Chongqing University, 55 Daxuecheng South Road, Shapingba, Chongqing 401331, PR China

Cancer cells metabolize glucose via anaerobic glycolysis, with lactate formed in the cytosol as the end-product. To avoid intercellular acidification, excessive lactate and proton are excreted by monocarboxylate transporters (MCTs), which are often overexpressed in different malignant cancers. Targeting the MCT-mediated lactate/proton efflux makes MCTs a potentially interesting anticancer target. Although X-ray co-crystal structures of human MCTs with inhibitors are not yet available, homology models have been established, which helped to rationalize the binding modes and the design of new MCT inhibitors. In this review, we discuss the structures and functions of MCTs as well as recently reported small-molecule MCTs inhibitors. We assess the current development of MCT inhibitors and highlight possible directions for future development.

Introduction

Cancer is the second leading cause of death globally. About 18.1 million people around the world have cancer and 9.6 million died as a result of it in 2018. Those figures will nearly double by 2040, with the greatest increase in low- and middle-income countries, where more than two-thirds of the world's cancers will occur [1]. Therefore, developing effective anticancer treatment has been an urgent need over the past decades, with a focus on the metabolic mechanisms of cancer cells being a particularly promising perspective. Normally, cells rely on mitochondrial oxidative phosphorylation (OXPHOS) to produce energy. When oxygen availability is limited, hypoxia can induce cells to use a fundamental metabolic adaptation to uncouple from aerobic respiration by using glycolysis to generate ATP [2], whereas adequate oxygen can reduce the catabolism of glucose and the accumulation of glycolysis products, such as L-lactate and pyruvate. This phenomenon is named the 'Pasteur effect' [3]. Moreover, a switch in cancer cells from a 'normal' metabolic profile to persistent cytosolic anaerobic glycolysis, was revealed by Otto Warburg, who referred to it as the 'Warburg effect' [4]. Anaerobic glycolysis contributes to the accumulation of lactate, which acts as a metabolic key player in cancer prognosis because of its important roles in maintaining an acidic tumor microenvironment (TME), reprogramming of energy metabolism, cell migration, angiogenesis, and immunomodulation [5,6]. The high lactate levels have significant clinical correlations with different cancers. For instance, metastatic tumors have significantly higher levels of lactate compared with non-metastatic tumors [7,8]. Therefore, strategies that modulate the intercellular and intracellular lactate levels could offer promising opportunities for developing new anticancer therapies [9].

Intracellular lactate level is dictated by membrane-bound human MCTs (*h*MCTs) (Fig. 1a), which comprise 14 transmembrane proteins (*h*MCT1–14) encoded by a family of genes, namely the solute carrier family 16 (SLC16) [10]. They function as transporters to carry a series of important endogenous or exogenous monocarboxylates across the plasma membrane [11]. Among the isoforms, *h*MCT1–4 are the most studied, and are responsible for the proton-linked transportation of L-lactate, pyruvate, and ketone bodies [12]. The overexpression of *h*MCT1–4 has been identified and disclosed in many different cancers, such as cervical carcinoma, glioblastoma, and breast, brain, colorectal, ovary, head and neck, lung, prostate, gastric, renal, adrenocortical, and soft tissue

Corresponding authors: Zhang, S.-L. (zhangsl@cqu.edu.cn), Tam, K.Y. (kintam@um.edu.mo)

https://doi.org/10.1016/j.drudis.2021.01.003

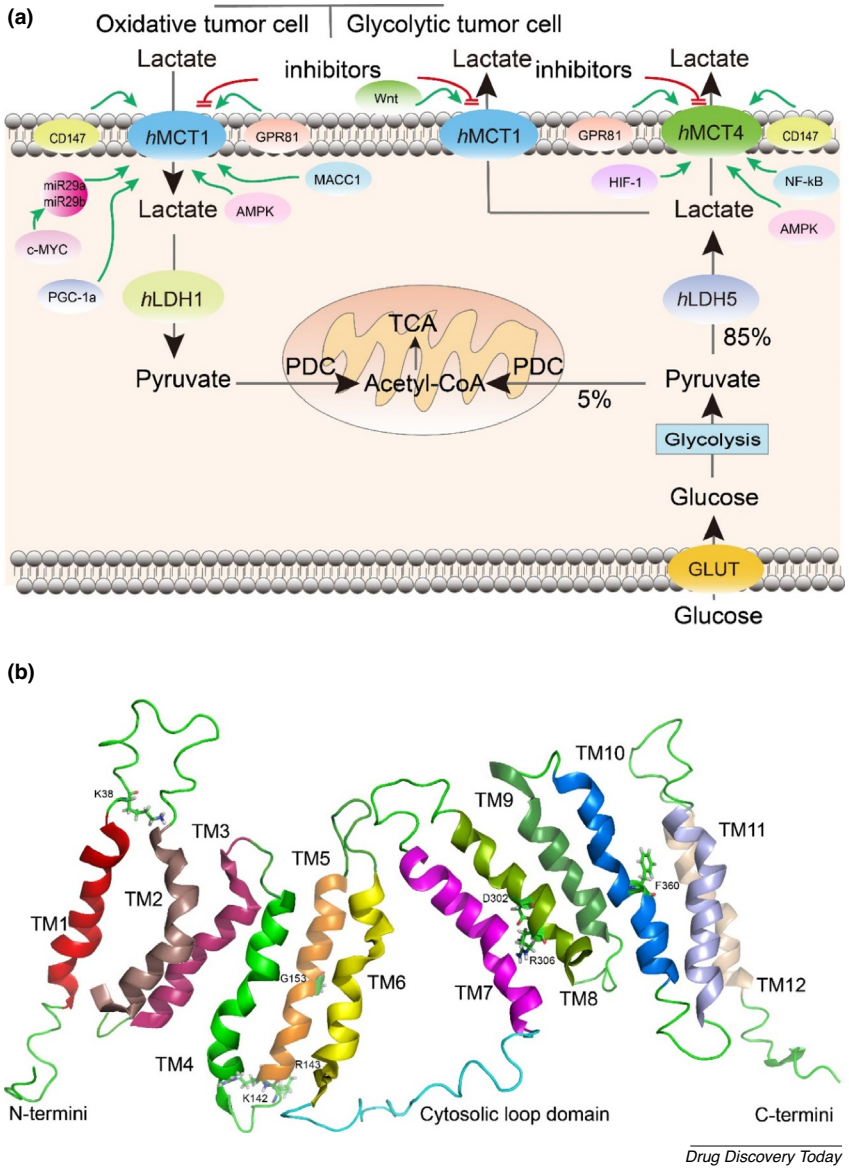

FIGURE 1

Human monocarboxylate transporters 1 and 4 (*h*MCT1 and *h*MCT4) in the exchange of lactate in tumor cells and the proposed structure of *h*MCT1. **(a)** *h*MCT1 and *h*MCT4 in the exchange of lactate in tumor cells and their regulation. **(b)** Proposed structure of *h*MCT1 derived from homology modeling and topological models. Twelve transmembrane domains (TMs) are drawn as helixes in different colors and denoted with numbers from left to right. The N and C termini are shown in green with the large cytosolic loop in cyan. The key residues (K38, K142, R143, G153, D302, R306, and F360) are labeled. For additional defintions, please see the main text.

cancers [13,14]. Extensive studies have revealed that overexpression of *h*MCT1–4 can promote cancer cell proliferation, migration, and tumor angiogenesis by facilitating lactate exchange in tumors. /ce:para>Upstream regulators of *h*MCTs include AMP-activated protein kinase (AMPK), peroxisome proliferator-activated receptor γ coactivator-1α (PGC-1α), G-protein-coupled receptor 81 (GPR81), *c*-Myc oncogene, hypoxia-activated transcription factors, nuclear factor-κB (NF-κB), miRNAs, chaperon proteins, and other modulators [15] (Fig. 1a). Inhibition of *h*MCTs by small-molecule inhibitors and small interfering (si)RNAs lead to lactate influx or efflux impairment. Both impairments can further result in apoptosis by inducing glucose deprivation or acidification of the cytosol in cancer cells, respectively [16,17]. Thus, the inhibition of *h*MCTs, especially *h*MCT1–4, could be a powerful approach for killing or at least greatly reducing the growth of cancer cells. Excitingly, a Phase I study with a first in class MCT1 inhibitor (AZD3965) suggested that therapeutic modulation of *h*MCTs was generally efficacious and well tolerated with observed metabolic effects in retinal function consistent with the inhibition of the intended target and the preclinical toxicology findings [18]. It is evident that the expression levels of different *h*MCT isoforms vary in different organs and cancer tissues, which could provide an extra dimension to optimize the design of selective of *h*MCT inhibitors for anticancer treatment.

Structures and functions of *h*MCT1–4

The designations of *h*MCT1–4 evolved gradually since 1994 as a result of progress in the molecular characterization of lactate transportation [19–22]. In general, *h*MCTs comprise 12 transmembrane domains (TMs) with intracellular C and N termini and a large cytosolic loop between TMs 6 and 7 [23] (Fig. 1b). The greatest variations are in the N and C termini and the large cytosolic loop, whereas the other TMs are highly conserved [11,12]. They share nearly 40% identity in amino acid sequences, two of which are known characteristics in *h*MCT family [24].

The four *h*MCTs have been characterized in terms of their differences in tissue distribution, function, and regulation. *h*MCT1 is ubiquitously expressed, except in β cells of the endocrine pancreas, facilitating L-lactic acid influx or efflux. *h*MCT2 is highly expressed in testis, spleen, heart, kidney, pancreas, skeletal muscle, brain, and leucocytes for taking up lactic acid. *h*MCT3, which can transport glycolytically derived lactic acid out of the retina, is detected only in retinal pigment epithelium and choroid plexus. *h*MCT4 is expressed preferentially in skeletal muscle, chondrocytes, leucocytes, testis, lung, brain, ovary, placenta, and heart, where it can export lactate to control intracellular pH homeostasis [12]. For correct expression, distribution, and function, the four isoforms need to interact with ancillary proteins, primarily basigin (CD147) or embigin (GP70), the TM domain of which lies adjacent to TM3 and TM6 of MCTs. MCT1, MCT3, and MCT4 mainly interact with basigin, which is more widely expressed in tissues compared with embigin, whereas MCT2 preferentially interacts with embigin [25,26].

These four isoforms show different binding affinities to L-lactic acid in the order: *h*MCT2 > *h*MCT1 > *h*MCT3 > *h*MCT4 [27]. The four isoforms transport L-lactic acid in a similar mechanism. In the structures of *h*MCT1–4, seven known key residues are conserved and involved in the translocation cycle of L-lactate (Fig. 1b). At the extracellular surface, K38 can promote a conformational change from a closed to open state by binding a proton, which forms an ionic pair with lactate [28]. Then, D302 and R306 in TM8 at the inner surface receive the proton and lactate in next step, respectively [29]; meanwhile, F360 in helices 10 and R306 have a crucial role in substrate selectivity by protruding into the channel as a steric hindrance [30]. By contrast, R143 and G153 in conserved helix 5 are also essential for transport function, and K142 and R143 are involved in stereoselectivity [31]. Residues near the R306 are not always conserved, indicating the possibility that these residues are involved in substrate recognition [32]. The loop between TMs 6 and 7 contributes to the substrate affinity of *h*MCTs [33]. In addition, R278 in TM8 of *h*MCT4 is also a crucial residue for substrate recognition [34], and H382 is a extracellular pH sensor in the pH-dependent regulation of the activity of *h*MCT4 [35].

Current development of small-molecular *h*MCT inhibitors with anticancer activities

Currently, there is no 3D co-crystal structures of *h*MCTs resolved by X-ray diffraction. However, the absence of crystallographic information did not prevented the development of a potent and selective inhibitor of *h*MCT1, AZD3965 (**12**), which advanced into Phase I clinical trials. Given the increasing number of *h*MCT1–4 inhibitors being reported, we summarize recent developments and generate new thoughts for supporting rational drug design.

Representative *h*MCT1, 2, and 4 inhibitors and their inhibitory activities data are listed in Fig. 2. These inhibitors can be roughly categorized into nonselective inhibitors and selective inhibitors. Nonselective inhibitors, such as stilbene sulfonates (**1**,**2**), quercetin (**3**), phloretin (**4**), α-cyano-4-hydroxy-cinnamic acid (CHC) (**5**), and p-chloromercuribenzene sulfonic acid (**6**), discovered during the 20th century, not only inhibit MCTs, but also affect other proteins. At the start of the 21 st century, some potent pyrimidinediones (**7**–**12**) were discovered as selective *h*MCT1 inhibitors by compound-led target identification and preliminary optimization [36–38]. The most potent and druggable pyrimidinedione, AZD3965 (**12**), underwent clinical evaluations in 2013 [39], whereas two new selective *h*MCT1 inhibitors (**13**, **14**) of coumarines were reported with good *in vitro* ADME profiles [40]. Herein, we focus on recently developed small-molecule MCT1 and 4 inhibitors, which can be classified based on their scaffolds as pyrimidinediones, pteridinones, coumarines, indole cyanoacrylic acids, 2-(indazol-3-yl-methoxy)-proponoic acids, (phenylsulfonyl-benzamido)benzoic acids, 2-(pyrrazol-3-yl-methyoxy)-propanoic acids, cinnamates, and others.

Selective MCT1 inhibitors

In 2014, Wang and colleagues reported a pteridinone scaffold (e.g., **8**, **9**) that was presented in many natural products and could be used for the design of new *h*MCT1 inhibitors [41]. By using a scaffold-hopping strategy, they designed and synthesized novel substituted pteridinones (**15**–**18**), which were able to selectively inhibit the growth of MCT1-expressing human lymphoma cells (EC_{50} = 37–150 nM).

In 2016, Gurrapu et al. reported 3-carboxy coumarins **19**–**23** with *N*,*N*-dialkylamino substitution at the 7-position as potent *h*MCT1 inhibitors with IC_{50} values ranging from 0.09 to 0.45 μM [42]. The *in vitro* Caco-2 permeability and metabolic stability of these compounds in mouse and human liver microsomes were also reported. One of these compounds, **19**, showed good absorption, metabolic stability, and a low drug efflux ratio, and was well tolerated in animal models. *In vivo* xenograft model studies showed that **19** exhibited superb efficacy and selectivity in MCT1-expressing tumors. In 2017, Tateishi et al. reported another two 3-carboxy coumarin analogs, **24** and **25**. One of these, **24**, was 55 times more active than the representative MCT inhibitor **5**. Their data suggested that **24** was transported into cells in an MCT1 expression-dependent manner [43].

By introduction of an indole ring, Samuel et al. designed and synthesized a series of indol-3-yl-cyanoacrylic acids and found that most of these indole cyanoacrylic acids were capable of inhibiting MCT1 well but did not show cytotoxicity in MCT4-overexpressed MDA-MB-231 cells. Two analogs, **26** and **27**, with good IC_{50} values against MCT1, deserve further studies, such as systemic toxicity and *in vivo* anticancer efficacy evaluations, in tumor xenograft models [44].

BAY-8002 **28**, with a 5-(phenylsulfonylbenzamido)benzoic acid scaffold, was discovered by Quanz and coworkers through a dedicated cell-based screen. Given that its inhibition potency against MCT2 was approximately fivefold lower compared with the MCT1 isoform, with no inhibition in MCT4-expressing oocytes, **28** was identified as a potent and specific *h*MCT1 inhibitor [45].

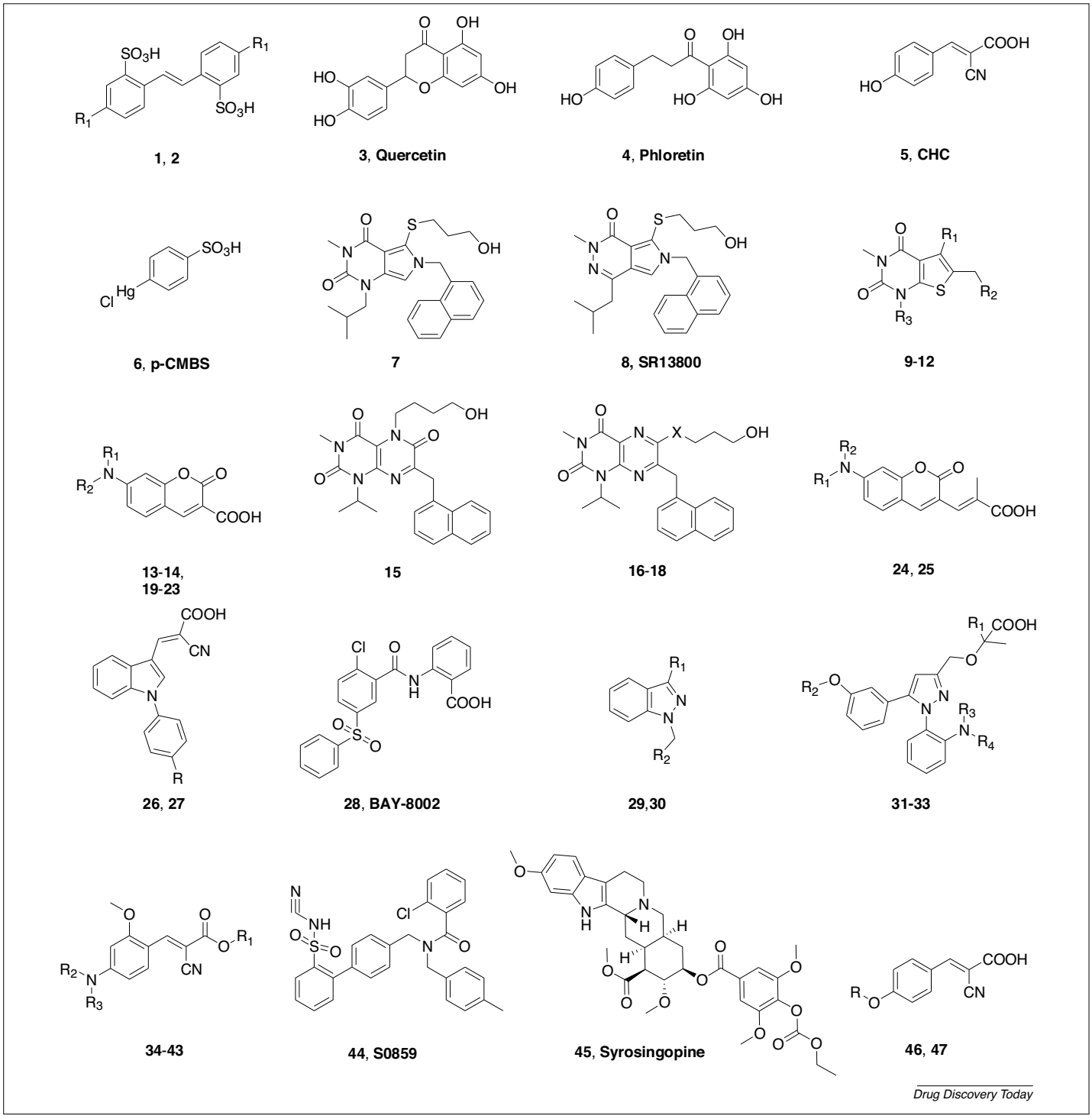

FIGURE 2

Structures of human monocarboxylate transporters 1 and 4 (*h*MCT1 and *h*MCT4) 4 inhibitors. The biological activity data was described as follows: **1**, **DIDS**, R_1 = isothiocyanato, MCT1 K_i = 39.5 mM; **2**, **DBDS**, R_1 = benzamido, MCT1 K_i = 22.4 mM; **3**, MCT1 K_i = 10 mM, MCT2 K_i = 5 mM, MCT4 K_i = 40 mM; **4**, MCT1 K_i = 5 mM, MCT2 K_i = 14 mM, MCT4 $K_{0.5}$ = 41 mM; **5**, MCT1 K_i = 166 mM, MCT2 K_i = 24 mM, MCT4 K_i = 994 mM; **6**, MCT1 K_i = 112 mM, MCT2 K_i = Ni, MCT4 $K_{0.5}$ = 21 mM; **7**, MCT1 K_i = 0.33 nM; **8**, MCT1 K_i = 0.1 nM; **9**, R_1 = -S-(CH2)3-OH, R_2 = (naphthalen-1-yl)methyl, R_3 = isobutyl, MCT1 K_i = 0.28 nM; **10**, R_1 = (R)-3-hydroxy pyrrolidine-1-carbonyl, R_2 = (quinolin-4-yl)methyl, R_3 = isobutyl, MCT1 K_i = 4.8 nM; **11**, **AR-C155858**, R_1 = (S)-4-hydroxy isoxazolidine-2-carbonyl, R_2 = (3,5-dimethyl-1H-pyrazol-4-yl)methyl, R_3 = isobutyl, MCT1 K_i = 1.2 nM, MCT2 K_i < 10 nM; **12**, **AZD3965**, R_1 = (S)-4-hydroxy-4-methyl-isoxazolidine-2-carbonyl, R_2 = (3-trifluoromethyl-5-methyl-1H-pyrazol-4-yl) methyl, R_3 = isopropyl, MCT1 K_i = 2 nM, MCT2 K_i = 20 nM; **13**, **7ACC1**, $R_1 = R_2$ = ethyl, $IC_{50\ lactate\ uptake}$ = 0.86 mM; **14**, **7ACC2**, R_1 = phenylmethyl, R_2 = methyl, $IC_{50\ lactate\ uptake}$ = 0.06 mM; **15**, MCT1 IC_{50} = 0.55 mM; **16**, X = S-CH2, MCT1 IC_{50} = 0.67 mM; **17**, X = CH2-CH2, MCT1 IC_{50} = 0.19 mM; **18**, X = *cis* -CH = CH-, MCT1 IC_{50} = 0.12 mM; **19**, $R_1 = R_2$ = benzyl, MCT1 IC_{50} = 0.09 mM; **20**, $R_1 + R_2$ = -$(CH_2)_4$-, MCT1 IC_{50} = 0.38 mM; **21**, $R_1 = R_2$ = propyl, MCT1 IC_{50} = 0.45 mM; **22**, $R_1 = R_2$ = allyl, MCT1 IC_{50} = 0.17 mM; **23**, $R_1 = R_2$ =prop-2-yn-1-yl, MCT1 IC_{50} = 0.21 mM; **24**, $R_1 = R_2$ = ethyl, MCT1 IC_{50} = 0.2 mM; **25**, R_1 = phenylmethyl, R_2 = methyl, MCT1 IC_{50} = 9.3 mM; **26**, R = H, MCT1 IC_{50} = 12.8 ± 2.6 nM, **27**, R = methoxyl, MCT1 IC_{50} = 21.9 ± 2.9 nM; **28**, MCT1, MCT2 K_i = nanomolar range; **29**, **lonidamine**, R_1 = -COOH, R_2 = 2,4-dichlorophenyl, MCT1 K_i = 36 mM, MCT2 K_i = 36 mM, MCT4 K_i = 40 mM; **30**, **bindarit**, R_1 = -CH_2O-C$(CH_3)_2$COOH, R_2 = phenyl, MCT1 IC_{50} > 500 mM,MCT4 K_i = 30.2 mM; **31**, R_1 = methyl, R_2 = cyclopropyl, $R_3 + R_4$ = -$(CH_2)_3$-, MCT1 IC_{50} = 29 mM, MCT4 IC_{50} = 2.1 nM;

Selective MCT4 inhibitors

In 2018, Yuya and coworkers identified a new potent 2-(indazol-3-yl-methoxy)-propanoic acid scaffold as a useful pharmacological tool for exploration of the physiological role of *h*MCT4. They found that lipid-lowering agents, such as bezafibrate, fenofibrate anion (the active metabolite of fenofibrate), and clinofibrate, could selectively inhibit the L-lactate transport activity of *h*MCT4, and the anti-inflammatory benzylindazole **29** showed potent inhibitory effects on *h*MCT4. By combining these two pre-existing scaffolds, the authors found that bindarit **30** ($K_i = 30.2 \pm 1.4$ μM for *h*MCT4) was a highly selective and noncompetitive inhibitor of *h*MCT4 [46].

In 2019, Parnell and his colleagues discovered potent heterocyclic *h*MCT4 inhibitors with good selectivity against *h*MCT1 (maximum value of ~180 000) from a screening campaign using 269 compounds, all with a 2-(pyrrazol-3-yl-methyoxy)-propanoic acid scaffold. In particular, **31–33** exhibited subnanomolar inhibition of *h*MCT4 and good pharmacokinetics properties [47].

Critchlow et al. reported a highly selective *h*MCT4 inhibitor AZD0095 (no structure information available) with a cellular activity of ~1–3 nM. Its selectivity to *h*MCT4 was >1000 times that of *h*MCT1. It was able to suppress myeloid infiltration as monotherapy and enhanced the antitumor activity of α-PD-1 or α-CTLA4 in combination treatment in MC-38 and EMT6 (*h*MCT-1 knockout) mouse syngeneic models [48].

Other less selective MCT inhibitors

Besides the aforementioned selective MCT1/4 inhibitors, some less selective MCT inhibitors have also been reported. In 2015, Gurrapu et al. designed a new series of cinnamates by introduction of p-*N*, *N*-dialkyl/diaryl-amino, and o-methoxy groups into an α-cyano-4-hydroxycinnamic acid template [49]. The most potent cinnamate, **34**, was converted to its sodium salt **35**, which was nontoxic, orally bioavailable, and efficacious as an antitumor agent in colorectal adenocarcinoma (WiDr cell line) xenograft models. Nine of these cinnamate analogs (**34**, **36–43**) were identified as potent and dual *h*MCT1 and four inhibitors with *h*MCT4 IC_{50} of 11–85 nM. The authors rationalized the potential MCT1 and MCT4-binding interactions of the representative compound by homology modeling and molecular docking [50].

In 2015, Heidtmann et al. reported that S0859 **44** was a protein inhibitor not only for sodium-bicarbonate cotransporters (NBC), but also for *h*MCT1, *h*MCT2, and *h*MCT4, with IC_{50} values of 4–10 μM [51]. In 2018, syrosingopine **45**, which sensitizes cancer cells to be killed by metformin, was identified as a dual *h*MCT1 and *h*MCT4 inhibitor (with 60-fold more potent activity against MCT4) [52,53]. In 2019, Nelson et al. discovered that silylated CHC derivatives **46** and **47** can reduce cancer cell proliferation by inhibiting MCT1. The novel silyl-CHC compounds were well tolerated in systemic toxicity and efficacy studies and exhibited good anticancer efficacy. Given that the two CHC derivatives showed improved cell proliferation inhibition against 4T1 and MDA-MB-231 cell lines, they were likely to be the dual inhibitors of *h*MCT1 and 4 [54].

Binding mechanism

Elucidating the binding mechanisms of *h*MCT inhibitors is useful for further lead optimization and drug discovery. Most potent and highly selective *h*MCT1 and 4 inhibitors are lactate competitive. Thus, the preliminary work of design is to identify suitable molecules to interact with the amino acid residues in the lactate-binding site of *h*MCT.

Given that MCT1 is found in most tissues without splice variants, Halestrap et al. proposed a modified 3D structure of rat MCT1 based on the published structure of the *Escherichia coli* glycerol-3-phosphate transporter [Protein Data Bank (PDB): 1PW4] [29,55]. Their model revealed that exofacial lysines might be responsible for the irreversible inhibition of MCT1 by DIDS and the cross-linking of MCT1 to embigin. This observation was consistent with the published site-directed mutagenesis data, suggesting a mechanism for the translocation cycle that involves Lys38 as well as Asp302 and Arg306, which have already been identified as important residues for lactate transport. Here, based on this modified 3D structure of MCT1, the binding patterns of the representative inhibitors in the active site of MCT1 were investigated.

In the structure of the DIDS-MCT1 complex (Fig. 3ai,bi), the isothiocyanate group in DIDS interacts with Lys38 of MCT1 by a hydrogen bond between the sulfur atom and amino group of Lys38. One of the sulfonic acid groups forms hydrogen bonds with the residues Thr41, Lys45, and Lys282, and interacts with Lys45 and Lys282 via a salt bridge. Another sulfonic acid group interacts with Asn279, Tyr280, Ser283, and Gly410 by hydrogen bonds, and offers an attractive charge interaction on Lys413. The alkyl chain between the aromatic rings in DIDS has a hydrophobic interaction with Ile50.

Different from DIDS, AR-C155858 is bound to MCT1 in a cation form in a different intracellular pocket in the C-terminal half of MCT1 involving TMs7-10 [56], which is related to substrate binding and translocation (Fig. 3aii,bii). The protonated nitrogen atom on the pyrazole ring forms two salt bridges with Asp302, a hydrogen bond with Gly148, and the cation-π interaction with Phe360, respectively. The isoxazolidine ring of AR-C155858 interacts with residues Gly31, Met151, and Ala152 by van der Waals forces. Alkyl groups on nitrogen and the pyrazole ring form hydrophobic interactions with Leu124, Leu363, Ala125, Ala 299, Ile30, Ala152, and Phe360. Key residues, Asp302, Arg306, and Phe360, in substrate binding and translocation of MCT1, are involved in this binding model.

As a potent and selective *h*MCT1 inhibitor, BAY-8002 was proved to bind to the same site in *h*MCT1 as AZD3965, an analog

32, R_1 = methyl, R_2 = cyclobutyl, $R_3 + R_4$ = -$(CH_2)_3$-, MCT1 IC_{50} = 26 mM, MCT4 IC_{50} = 0.83 nM; **33**, R_1 = (R)-ethyl, R_2 = cyclopropyl, $R_3 + R_4$ = -$(CH_2)_3$-, MCT1 IC_{50} = 64 mM, MCT4 IC_{50} = 0.36 nM; **34**, R_1 = H, $R_2 = R_3$ = phenyl, MCT1 IC_{50} = 8 nM, MCT4 IC_{50} = 23 nM; **35**, R_1 = Na, $R_2 = R_3$ = phenyl, MCT1 IC_{50} = 11 nM; **36**, R_1 = H, $R_2 = R_3$ = propyl, MCT1 IC_{50} = 12 nM, MCT4 IC_{50} = 11 nM; **37**, R_1 = H, $R_2 = R_3$ = allyl, MCT1 IC_{50} = 29 nM, MCT4 IC_{50} = 28 nM; **38**, R_1 = H, $R_2 = R_3$ = butyl, MCT1 IC_{50} = 9 nM, MCT4 IC_{50} = 14 nM; **39**, R_1 = H, $R_2 = R_3$ = isobutyl, MCT1 IC_{50} = 11 nM, MCT4 IC_{50} = 17 nM; **40**, R_1 = H, $R_2 = R_3$ = pentyl, MCT1 IC_{50} = 34 nM, MCT4 IC_{50} = 85 nM; **41**, R_1 = H, $R_2 + R_3$ = -$(CH_2)_4$-, MCT1 IC_{50} = 48 nM, MCT4 IC_{50} = 53 nM; **42**, R_1 = H, $R_2 + R_3$ = -$(CH_2)_6$-, MCT1 IC_{50} = 25 nM, MCT4 IC_{50} = 58 nM; **43**, R_1 = H, $R_2 = R_3$ = benzyl, MCT1 IC_{50} = 37 nM, MCT4 IC_{50} = 32 nM; **44**, MCT1 IC_{50} = 10 mM, MCT2 IC_{50} = 4 mM, MCT4 IC_{50} = 5 mM; **45**, MCT1 IC_{50} = 2500 mM, MCT4 IC_{50} = 40 nM; **46**, R = TBDPS-, MCT1 IC_{50} = 408 nM; **47**, R = TBDPSO$(CH_2)_2$-, MCT1 IC_{50} = 97 nM.

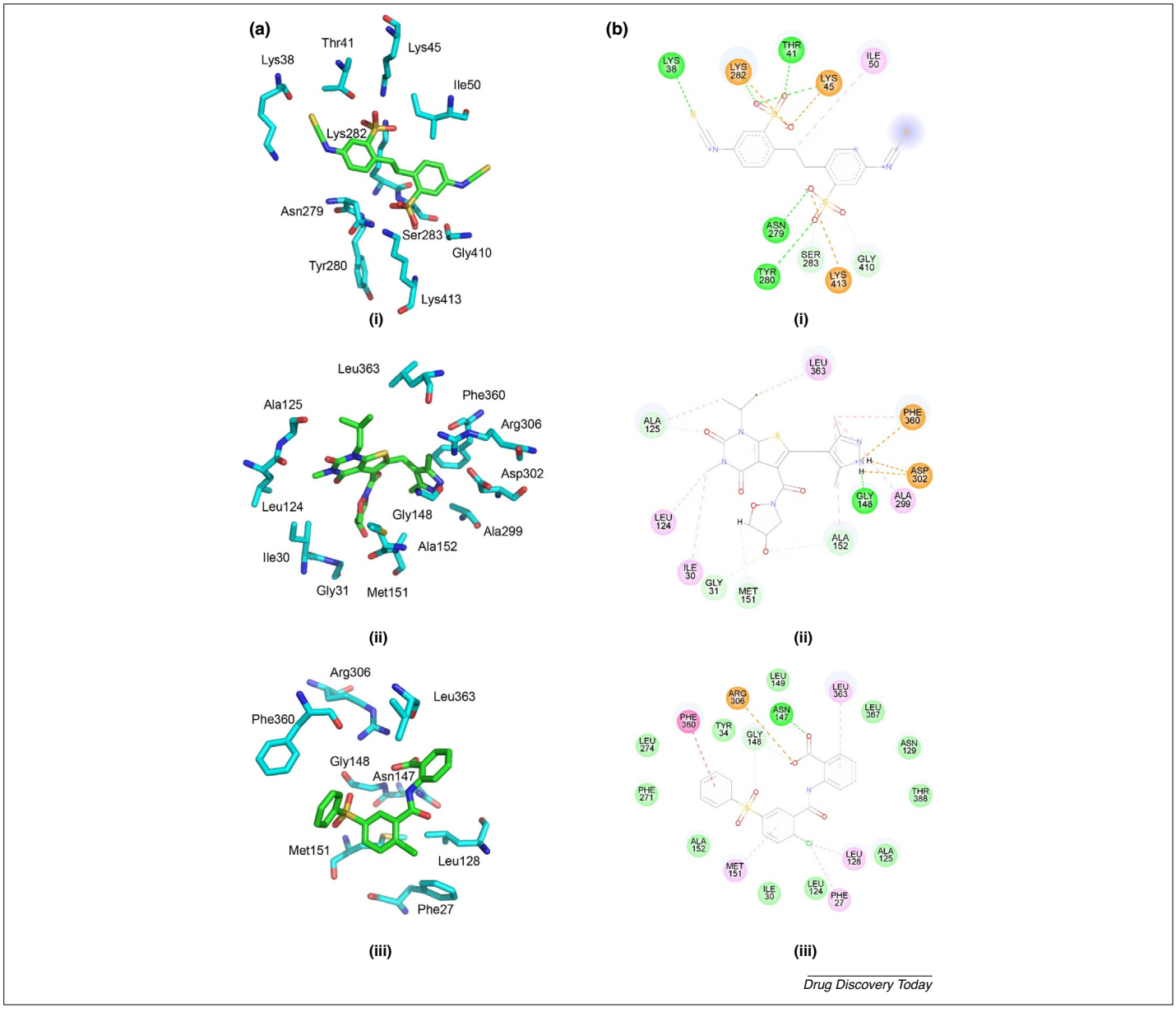

FIGURE 3

Binding modes of representative monocarboxylate transporter 1 (MCT1) inhibitors. **(a)** The key residues in the binding site of three inhibitor–MCT1 complexes [(i) DIDS, (ii) AR-C155858, (iii) BAY-8002). **(b)** Schematic representations of the interactions between MCT1 and inhibitors [(i) DIDS, (ii) AR-C155858, (iii) BAY-8002). Figures generated by the Discovery Studio 2017 *R2*.

of AR-C155858, in radioactive-binding assays [45]. According to the structure of the BAY-8002-MCT1 complex (Fig. 3aiii, biii), the carboxyl group and sulfone group have crucial roles in the connection between BAY-8002 and the hinge region. The carboxyl oxygen atom forms a hydrogen bond with the amide NH of Asn147 and a strong attractive charge interaction with Arg306, and interacts with Gly148 via van der Waals force, whereas the sulfone group interacts with Gly148 at the same side. One of the aryls in the structure of BAY-8002 forms a π-π T-shaped interaction with Phe360, and the other two aryls form π-alkyl interactions with Met151 and Leu363, respectively. The chlorine atom is also involved in the binding model by interactions with residues Phe127 and Leu128.

To rationalize the binding modes of *h*MCT4 inhibitors, a homology model of *h*MCT4 is necessary. Recently, the 3D structures of *Syntrophobacter fumaroxidans* monocarboxylate transporters (SfMCT) (PDB: 6HCL) and *h*MCT2 (PDB: 7BP3) became available [57,58]. Although the known cryo-electron microscopy (cryo-EM) structure of *h*MCT2 is more homologous than that of SfMCT, its closed conformation limits its use in drug design. The 3D crystal structure of SfMCT shares 22% amino acid sequence identity and 41% sequence similarity with *h*MCT4, and has a suitable outward-open conformation for ligand binding. Hence, a homology model of *h*MCT4 was built by using the 3D structures of SfMCT as the template and used to investigate the binding modes of representative *h*MCT4 inhibitors.

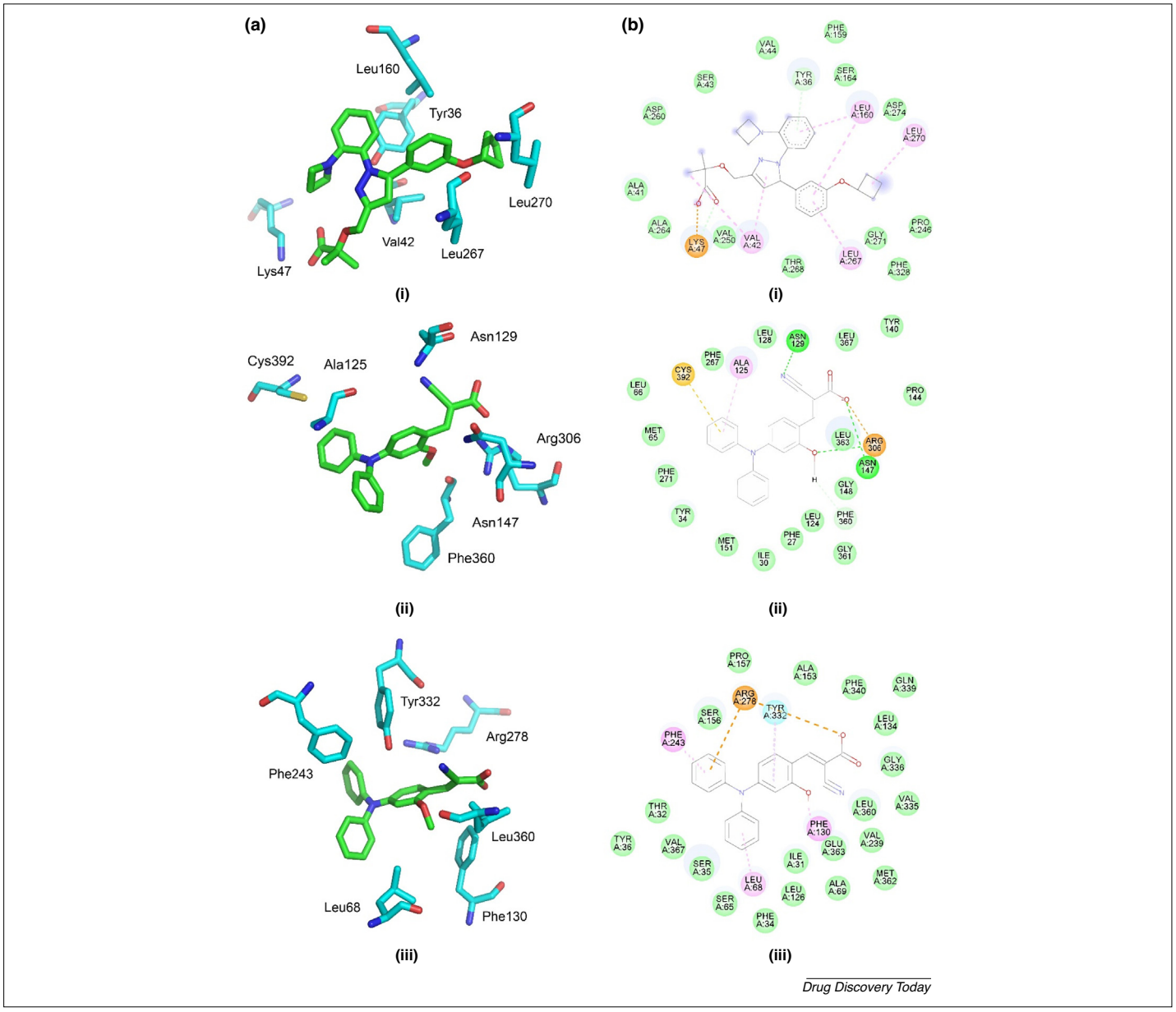

FIGURE 4

Binding modes of representative monocarboxylate transporter 4 (MCT4) inhibitors and MCT1/4 dual inhibitors. **(a)** Key residues in the binding site of three inhibitor–MCT4 complexes [(i) 2-(pyrrazol-3-yl-methyoxy)-propanoic acid **32**-MCT4, (ii) *N*,*N*-diphenyl-4-amino-cinnamate **34**-MCT1, (iii) *N*,*N*-diphenyl-4-amino-cinnamate **34**-MCT4). **(b)** Schematic representations of the interactions between inhibitors and MCTs [(i) 2-(pyrrazol-3-yl-methyoxy)-propanoic acid **32** and MCT4, (ii) *N*,*N*-diphenyl-4-amino-cinnamate **34** and MCT1, (iii) *N*,*N*-diphenyl-4-amino-cinnamate **34** and MCT4). Figures generated by the Discovery Studio 2017 *R2*.

One of the known *h*MCT4 inhibitors, 2-(pyrrazol-3-yl-methyoxy)-propanoic acid **32,** binds to *h*MCT4 in a bulky cavity (Fig. 4ai,bi). There are two four-membered rings in the scaffold. These hydrophobic ring systems enable strong nonpolar interactions with the binding pockets. Moreover, its large molecular volume could be the reason for its outstanding selectivity against *h*MCT1. In the structure of the propanoic acid **32**–MCT4 complex, the carboxy of propanoic acid **32** forms a salt bridge and a hydrogen bond with Lys47. One of the methyls and the pyrazole ring interact with Val42 via alkyl- and π-alkyl interactions. The two phenyls and the cyclobutyl occupy a broad hydrophobic area by alkyl and π-alkyl interactions with Leu160 and Leu270. The phenyl on the nitrogen interacts with Tyr36 as a hydrogen bond acceptor.

The potent dual inhibitor of *h*MCT1 and *h*MCT4, *N*,*N*-diphenyl-4-amino-cinnamate **34** binds to *h*MCT1 and *h*MCT4 at a substrate recognition pocket, respectively. By comparing the binding of AR-C155858 (Fig. 3aii,bii) and *N*,*N*-diphenyl-4-amino-cinnamate **34** (Fig. 4aii,bii) to MCT1, it can be seen that they bind to the same pocket. Owing to their different structures, especially the functional groups, they exhibit different binding modes. In the binding mode of *N*,*N*-diphenyl-4-amino-cinnamate **34,** the methoxyl, carboxyl, and cyano groups interact with the residues Asn129, Asn147, and Arg306 by hydrogen bonds. Other contributions from

the carboxyl and methoxy of cinnamate **34** are the salt bridge and van der Waals force interactions with Arg306 and Phe360, respectively. Similar to AR-C155858, cinnamate **34** also has a scaffold that shows hydrophobic interactions with closing residues Ala125 and Cys392 by π-alkyl and π-sulfur interactions, respectively. In the cinnamate **34**-*h*MCT4 complex (Fig. 4aiii,biii), one of the phenyls on the nitrogen atom forms π-alkyl interactions with Leu68. Another phenyl on nitrogen and carboxyl interacts with Arg278, the key residue of substrate recognition, via π-cation and attractive charge interactions, respectively. The phenyl in the main chain of cinnamate interacts with Tyr332 as a hydrogen bond acceptor. The methoxyl group interacts with the residues Phe130 via alkyl-π interactions. The cyano group stretches into a hydrophobic domain, which comprises Phe130, Leu360, and Gly363.

Concluding remarks and future directions

Over the past decades, *h*MCTs have been identified as a potential target for different cancers, and several potent MCTs inhibitors with nanomolar range IC_{50} values have been discovered. Some are under or going into clinical trials. However, the development of inhibitors against these membrane bound targets is more challenging than with other protein targets, partly because of the lack of 3D crystal structures of the proteins involved. By contrast, the universal expression of the *h*MCTs and their unclear versatility of functions could lead to off-target effects and unexpected toxicity *in vivo* [45]. For example, as one of the important physiological functions of *h*MCT1, transport of 5-oxoproline, which is an analog of glutamate, in the brain was reported recently [59]. These issues make the discovery of drug-targeting *h*MCTs for cancer treatment difficult and time-consuming. With technological advancements in cryo-EM, molecular modeling technologies, site-directed mutagenesis, and other modeling protocols, more precise structural information on the targets will become available, which will aid the rational molecular design of potent and selective *h*MCTs inhibitors.

In the future, as we develop a better understanding of the physiological functions of *h*MCTs, the emphasis of anticancer drug design could be directed to the reduction of off-target effects of *h*MCT1 inhibitors. Meanwhile, because *h*MCT4 has a more specific expression in normal organs and pathological tissues and more simple functions compared with *h*MCT1 [60], the design and discovery of potent and selective inhibitors against *h*MCT4 for anticancer treatment is likely to be an exciting new direction in medicinal chemistry.

Acknowledgments

We acknowledge financial support from the Science and Technology Development Fund, Macau SAR (File no. 0057/2018/A2) and University of Macau (File no. MYRG2019-00034-FHS).

References

1 Ilbawi, A. and Varghese, C. (2020) *WHO Report on Cancer: Setting Priorities, Investing Wisely and Providing Care for All*. WHO
2 Dang, C.V. and Semenza G.L, G.L. (1999) Oncogenic alterations of metabolism. *Trends Biochem. Sci.* 24, 68–72
3 Wu, R. and Racker, E. (1959) Regulatory mechanisms in carbohydrate metabolism. IV. Pasteur effect and Crabtree effect in ascites tumor cells. *J. Biol. Chem.* 234, 1036–1041
4 Semenza, G.L. *et al.* (2001) The metabolism of tumours': 70 years later. *Novartis Found Symp.* 240, 251–260 discussion 260–254
5 Hirschhaeuser, F. *et al.* (2011) Lactate: a metabolic key player in cancer. *Cancer Res.* 71 (22), 6921–6925
6 Gottfried, E. *et al.* (2012) Tumor metabolism as modulator of immune response and tumor progression. *Semin. Cancer Biol.* 22, 335–341
7 Schwickert, G. *et al.* (1995) Correlation of high lactate levels in human cervical cancer with incidence of metastasis. *Cancer Res.* 55 (21), 4757–4759
8 Walenta, S. *et al.* (1997) Correlation of high lactate levels in head and neck tumors with incidence of metastasis. *Am. J. Pathol.* 150, 409–415
9 Doherty, J.R. *et al.* (2014) Blocking lactate export by inhibiting the Myc target MCT1 Disables glycolysis and glutathione synthesis. *Cancer Res.* 74, 908–920
10 Kennedy, K.M. and Dewhirst, M.W. (2010) Tumor metabolism of lactate: the influence and therapeutic potential for MCT and CD147 regulation. *Future Oncol.* 6, 127–148
11 Halestrap, A.P. and Meredith, D. (2004) The SLC16 gene family-from monocarboxylate transporters (MCTs) to aromatic amino acid transporters and beyond. *Pflugers Arch.* 447, 619–628
12 Halestrap, A.P. and Wilson, M.C. (2012) The monocarboxylate transporter family–role and regulation. *IUBMB Life* 64, 109–119
13 Perez-Escuredo, J. *et al.* (2016) Monocarboxylate transporters in the brain and in cancer. *Biochim. Biophys. Acta* 1863, 2481–2497
14 Park, S.J. *et al.* (2018) An overview of MCT1 and MCT4 in GBM: small molecule transporters with large implications. *Am. J. Cancer Res.* 8, 1967–1976
15 Payen, V.L. *et al.* (2020) Monocarboxylate transporters in cancer. *Mol. Metab.* 33, 48–66
16 Sonveaux, P. *et al.* (2008) Targeting lactate-fueled respiration selectively kills hypoxic tumor cells in mice. *J. Clin. Invest.* 118, 3930–3942
17 Todenhofer, T. *et al.* (2018) Selective inhibition of the lactate transporter MCT4 reduces growth of invasive bladder cancer. *Mol. Cancer Ther.* 17, 2746–2755
18 Halford, S.E.R. *et al.* (2017) A first-in-human first-in-class (FIC) trial of the monocarboxylate transporter 1 (MCT1) inhibitor AZD3965 in patients with advanced solid tumours. *J. Clin. Oncol.* 35 (15_Suppl), 2516–2516
19 Garcia, C.K. *et al.* (1994) Molecular characterization of a membrane transporter for lactate, pyruvate, and other monocarboxylates - implications for the Cori cycle. *Cell* 76, 865–873
20 Garcia, C.K. *et al.* (1995) cDNA cloning of Mct2, a 2nd monocarboxylate transporter expressed in different cells than Mct1. *J. Biol. Chem.* 270, 1843–1849
21 Grollman, E.F. *et al.* (2000) Determination of transport kinetics of chick MCT3 monocarboxylate transporter from retinal pigment epithelium by expression in genetically modified yeast. *Biochemistry* 39 (31), 9351–9357
22 Price, N.T. *et al.* (1998) Cloning and sequencing of four new mammalian monocarboxylate transporter (MCT) homologues confirms the existence of a transporter family with an ancient past. *Biochem. J.* 329, 321–328
23 Poole, R.C. *et al.* (1996) Studies of the membrane topology of the rat erythrocyte H +/lactate cotransporter (MCT1). *Biochem. J.* 320, 817–824
24 Halestrap, A.P. and Price, N.T. (1999) The proton-linked monocarboxylate transporter (MCT) family: structure, function and regulation. *Biochem. J.* 343, 281–299
25 Philp, N.J. *et al.* (2003) Loss of MCT1, MCT3, and MCT4 expression in the retinal pigment epithelium and neural retina of the 5A11/basigin-null mouse. *Invest. Ophthalmol. Visual Sci.* 44, 1305–1311
26 Ovens, M.J. *et al.* (2010) The inhibition of monocarboxylate transporter 2 (MCT2) by AR-C155858 is modulated by the associated ancillary protein. *Biochem. J.* 431, 217–225
27 Halestrap, A.P. (2012) The monocarboxylate transporter family–structure and functional characterization. *IUBMB Life* 64, 1–9
28 Yamaguchi, A. *et al.* (2020) Extracellular lysine 38 plays a crucial role in pH–dependent transport via human monocarboxylate transporter 1. *Biochim. Biophys. Acta Biomembr.* 1862, 183068
29 Manoharan, C. *et al.* (2006) The role of charged residues in the transmembrane helices of monocarboxylate transporter 1 and its ancillary protein basigin in determining plasma membrane expression and catalytic activity. *Mol. Membr. Biol.* 23, 486–498
30 Rahman, B. *et al.* (1999) Helix 8 and helix 10 are involved in substrate recognition in the rat monocarboxylate transporter MCT1. *Biochemistry* 38 (35), 11577–11584

31 Galic, S. *et al.* (2003) The loop between helix 4 and helix 5 in the monocarboxylate transporter MCT1 is important for substrate selection and protein stability. *Biochem. J.* 376, 413–422

32 Nancolas, B. *et al.* (2015) Identification of key binding site residues of MCT1 for AR-C155858 reveals the molecular basis of its isoform selectivity. *Biochem. J.* 466, 177–188

33 Futagi, Y. *et al.* (2017) The flexible cytoplasmic loop 3 contributes to the substrate affinity of human monocarboxylate transporters. *Biochimica. Et Biophysica. Acta-Biomembranes* 1859, 1790–1795

34 Sasaki, S. *et al.* (2013) Crucial residue involved in L-lactate recognition by human monocarboxylate transporter 4 (hMCT4). *PLoS One* 8, e67690

35 Sasaki, S. *et al.* (2015) Involvement of histidine residue His382 in pH regulation of MCT4 activity. *PLoS One* 10, e0122738

36 Murray, C.M. *et al.* (2005) Monocarboxylate transporter MCT1 is a target for immunosuppression. *Nat. Chem. Biol.* 1, 371–376

37 Guile, S.D. *et al.* (2006) Potent blockers of the monocarboxylate transporter MCT1: Novel immunomodulatory compounds. *Bioorg. Med. Chem. Lett.* 16, 2260–2265

38 Guile, S.D. *et al.* (2007) Optimization of monocarboxylate transporter 1 blockers through analysis and modulation of atropisomer interconversion properties. *J. Med. Chem.* 50, 254–263

39 Frautschy, S.A. and Cole, G.M. (2010) Why pleiotropic interventions are needed for Alzheimer's disease. *Mol. Neurobiol.* 41 (2-3), 392–409

40 Draoui, N. *et al.* (2013) Synthesis and pharmacological evaluation of carboxycoumarins as a new antitumor treatment targeting lactate transport in cancer cells. *Bioorg. Med. Chem.* 21 (22), 7107–7117

41 Wang, H. *et al.* (2014) Synthesis and structure activity relationships of pteridine dione and trione monocarboxylate transporter 1 inhibitors. *J. Med. Chem.* 57 (17), 7317–7324

42 Gurrapu, S. *et al.* (2016) Coumarin carboxylic acids as monocarboxylate transporter 1 inhibitors: In vitro and *in vivo* studies as potential anticancer agents. *Bioorg. Med. Chem. Lett.* 26 (14), 3282–3286

43 Tateishi, H. *et al.* (2017) Synthesis and evaluation of C-11-labeled coumarin analog as an imaging probe for detecting monocarboxylate transporters expression. *Bioorg. Med. Chem. Lett.* 27 (21), 4893–4897

44 Samuel, K. (2016). Synthesis and evaluation of indole cyanoacrylic acids as anticancer agents. Retrieved from the University of Minnesota Digital Conservancy, https://hdl.handle.net/11299/185070.

45 Quanz, M. *et al.* (2018) Preclinical efficacy of the novel monocarboxylate transporter 1 inhibitor BAY-8002 and associated markers of resistance. *Mol. Cancer Ther.* 17, 2285–2296

46 Futagi, Y. *et al.* (2018) Identification of a selective inhibitor of human monocarboxylate transporter 4. *Biochem. Biophys. Res. Commun.* 495, 427–432

47 Parnell, K.M. et al. Vettore LLC. Heterocyclic inhibitors of MCT4. US10214492.

48 Critchlow, S.E. *et al.* (2019) Reversing lactate-driven immunosuppression using the novel, potent and selective MCT4 inhibitor AZD0095. *Cancer Res.* 79 (Suppl), 1207

49 Gurrapu, S. *et al.* (2015) Monocarboxylate transporter 1 inhibitors as potential anticancer agents. *ACS Med. Chem. Lett.* 6, 558–561

50 Jonnalagadda, S. *et al.* (2019) Novel N,N-dialkyl cyanocinnamic acids as monocarboxylate transporter 1 and 4 inhibitors. *Oncotarget* 10 (24), 2355–2368

51 Heidtmann, H. *et al.* (2015) Inhibition of monocarboxylate transporter by N-cyanosulphonamide S0859. *Eur. J. Pharmacol.* 762, 344–349

52 Benjamin, D. *et al.* (2016) Syrosingopine sensitizes cancer cells to killing by metformin. *Sci. Adv.* 2, e1601756

53 Benjamin, D. *et al.* (2018) Dual inhibition of the lactate transporters MCT1 and MCT4 is synthetic lethal with metformin due to NAD plus depletion in cancer cells. *Cell Rep.* 25, 3047–3058

54 Nelson, G.L. *et al.* (2019) Development of novel silyl cyanocinnamic acid derivatives as metabolic plasticity inhibitors for cancer treatment. *Sci. Rep.* 9, 18266

55 Wilson, M.C. *et al.* (2009) Studies on the DIDS-binding site of monocarboxylate transporter 1 suggest a homology model of the open conformation and a plausible translocation cycle. *J. Biol. Chem.* 284 (30), 20011–20021

56 Ovens, M.J. *et al.* (2010) AR-C155858 is a potent inhibitor of monocarboxylate transporters MCT1 and MCT2 that binds to an intracellular site involving transmembrane helices 7-10. *Biochem. J.* 425, 523–530

57 Zhang, B. *et al.* (2020) Cooperative transport mechanism of human monocarboxylate transporter 2. *Nat. Commun.* 11, 2429

58 Bosshart, P.D. *et al.* (2019) Mechanistic basis of L–lactate transport in the SLC16 solute carrier family. *Nat. Commun.* 10, 2649

59 Sasaki, S. *et al.* (2015) Functional characterization of 5-oxoproline transport via SLC16A1/MCT1. *J. Biol. Chem.* 290, 2303–2311

60 Contreras-Baeza, Y. *et al.* (2019) Monocarboxylate transporter 4 (MCT4) is a high affinity transporter capable of exporting lactate in high-lactate microenvironments. *J. Biol. Chem.* 294 (52), 20135–20147